Photodissociation of benzene under collision-free conditions: An ab initio/Rice–Ramsperger–Kassel–Marcus study

V. V. Kislov, T. L. Nguyen, A. M. Mebel, S. H. Lin, and S. C. Smith

Citation: The Journal of Chemical Physics **120**, 7008 (2004); doi: 10.1063/1.1676275

View online: http://dx.doi.org/10.1063/1.1676275

View Table of Contents: http://scitation.aip.org/content/aip/journal/jcp/120/15?ver=pdfcov

Published by the AIP Publishing

Photodissociation of benzene under collision-free conditions: An *ab initio*/Rice–Ramsperger–Kassel–Marcus study

V. V. Kislov[a] and T. L. Nguyen[b]
Institute of Atomic and Molecular Sciences, Academia Sinica, P.O. Box 23-166, Taipei 10764, Taiwan

A. M. Mebel[c]
Department of Chemistry and Biochemistry, Florida International University, Miami, Florida 33199 and Institute of Atomic and Molecular Sciences, Academia Sinica, P.O. Box 23-166, Taipei 10764, Taiwan

S. H. Lin
Institute of Atomic and Molecular Sciences, Academia Sinica, P.O. Box 23-166, Taipei 10764, Taiwan

S. C. Smith
Computational Molecular Science Group, Department of Chemistry, University of Queensland, St. Lucia, Qld 4072, Australia

(Received 29 September 2003; accepted 22 January 2004)

The *ab initio*/Rice–Ramsperger–Kassel–Marcus (RRKM) approach has been applied to investigate the photodissociation mechanism of benzene at various wavelengths upon absorption of one or two UV photons followed by internal conversion into the ground electronic state. Reaction pathways leading to various decomposition products have been mapped out at the G2M level and then the RRKM and microcanonical variational transition state theories have been applied to compute rate constants for individual reaction steps. Relative product yields (branching ratios) for C_6H_5+H, $C_6H_4+H_2$, $C_4H_4+C_2H_2$, $C_4H_2+C_2H_4$, $C_3H_3+C_3H_3$, $C_5H_3+CH_3$, and $C_4H_3+C_2H_3$ have been calculated subsequently using both numerical integration of kinetic master equations and the steady-state approach. The results show that upon absorption of a 248 nm photon dissociation is too slow to be observable in molecular beam experiments. In photodissociation at 193 nm, the dominant dissociation channel is H atom elimination (99.6%) and the minor reaction channel is H_2 elimination, with the branching ratio of only 0.4%. The calculated lifetime of benzene at 193 nm is about 11 μs, in excellent agreement with the experimental value of 10 μs. At 157 nm, the H loss remains the dominant channel but its branching ratio decreases to 97.5%, while that for H_2 elimination increases to 2.1%. The other channels leading to $C_3H_3+C_3H_3$, $C_5H_3+CH_3$, $C_4H_4+C_2H_2$, and $C_4H_3+C_2H_3$ play insignificant role but might be observed. For photodissociation upon absorption of two UV photons occurring through the neutral ''hot'' benzene mechanism excluding dissociative ionization, we predict that the C_6H_5+H channel should be less dominant, while the contribution of $C_6H_4+H_2$ and the $C_3H_3+C_3H_3$, $CH_3+C_5H_3$, and $C_4H_3+C_2H_3$ radical channels should significantly increase. © *2004 American Institute of Physics.*
[DOI: 10.1063/1.1676275]

I. INTRODUCTION

Benzene is a prototype aromatic molecule and its photochemical behavior has attracted a significant attention in recent years. Now it is generally recognized that nonadiabatic processes play an important role in photodissociation dynamics of benzene.[1–4] For instance, the hot-benzene mechanism has been proposed to account for the observed experimental results.[5,6] The hot benzene is highly vibrationally excited ground electronic state benzene, which is produced by internal conversion from the electronically excited singlet states populated after photoexcitation. Lifetimes of the first and second excited states of benzene have been measured using pump–probe methods with femtosecond lasers.[7,8] Benzene molecules in the S_2 state excited by 200 nm light were shown to have a decay lifetime of about 40 fs. It is believed that the S_2 state mainly decays to the lower S_1 and S_0 electronic states. From the same measurement, the decay of the vibrationally excited S_1 levels to the S_0 state was reported to be within 5–10 ps. Recently, the decay lifetime of benzene excited by 155 nm light was determined as 70 fs.[9] All these results indicate that electronically excited benzene molecules decay very rapidly via fast internal conversion to lower electronic state (and eventually to the ground electronic state), and the ''hot'' benzene mechanism is adequate. Therefore, the photodissociation dynamics can be described in terms of the ground electronic state potential energy surface (PES).

Early experiments on the photolysis of benzene assigned the major products as fulvene,[5,10–12] 1,3-hexadien-5-yne,[6,13] and polymers, with the minor products including methane,

[a]Permanent address: Institute of Solution Chemistry of Russian Academy of Sciences, Akademicheskaya St., 1, Ivanovo, 153045, Russia.
[b]Present address: Division of Physical and Analytical Chemistry, Department of Chemistry, University of Leuven, Belgium.
[c]Author to whom correspondence should be addressed. Electronic mail: mebela@fiu.edu

ethane, ethylene, hydrogen, and acetylene.[10,14] However, in those experiments the primary photolysis products could undergo collisional deactivation with the buffer gas and also participate in secondary reactions. The use of the molecular beam technique in recent years allowed the researches to obtain a more clear view on the primary photodissociation dynamics under collision-free conditions. For instance, in 1990 Yokoyama *et al.* detected C_6H_5+H, $C_6H_4+H_2$, and, surprisingly, $C_5H_3+CH_3$ as primary products of benzene photodissociation at 193 and 248 nm.[15] Recently, Ni *et al.* used a more advanced molecular beam apparatus to investigate the photodissociation reaction at 193 nm and found the following products: C_6H_5+H, $C_6H_4+H_2$, $C_5H_3+CH_3$, and $C_4H_3+C_2H_3$.[16,17] This means that all kinds of cracking patterns of the C_6 aromatic ring are possible providing sufficient energy, including C_5/C, C_4/C_2, and C_3/C_3 with various distributions of hydrogen atoms between the fragments. Ni *et al.* also showed that the H atom elimination channel comes from one-photon absorption, while 2H or H_2, CH_3, C_2H_3 elimination channels come from two-photon absorption.[17] It should be noted that Ni *et al.* applied the multimass ion imaging technique, which allowed them to distinguish between dissociative ionization and dissociation of neutral benzene. For the former, the products gave disk-like images, on the contrary to line shape images for the latter. The photodissociation of benzene at 193 and 157 nm has been also investigated in the collisionless molecular beam conditions using the photofragment translational spectroscopic technique and the results confirmed that the H elimination originates from one-photon absorption and is a direct dissociation channel, while the H_2 and CH_3 eliminations are two-photon processes.[18,19]

For the hot-benzene photodissociation mechanism, *ab initio* studies of the reaction pathways on the ground state PES can elucidate the dissociation and isomerization mechanisms. Using the *ab initio* energies and molecular parameters for various intermediates and transition states, we can apply then the Rice–Ramsperger–Kassel–Marcus (RRKM) [or variational transition state theory (VTST)] approach in order to predict individual reaction rate coefficients and relative branching ratios of different products as functions of the available internal energy determined by the excitation wavelength. It is important to note that the statistical theory, such as RRKM, can be applied to rate constant calculations if the system has a sufficient time to undergo intramolecular vibrational relaxation (IVR), i.e., IVR must be faster than the isomerization and/or dissociation processes. For the medium-size molecules like benzene, IVR is supposed to occur on a picosecond time scale and therefore, as long as the reaction rate constants do not exceed the $10^{13}\,s^{-1}$ limit, the RRKM theory is applicable.

Over the recent years, we have studied various isomerization and dissociation pathways of benzene employing high level *ab initio* and density functional calculations.[20–23] The PES of benzene have been also investigated before by Miller and Melius,[24,25] Bettinger *et al.*,[26] and most recently by Miller and Klippenstein in conjunction with RRKM calculations of temperature/pressure dependent rate constants for the recombination of two propargyl radicals.[27,28] In this paper, we used the *ab initio* PES for the C_6H_6 species and molecular parameters to carry out microcanonical RRKM calculations of the dissociation and isomerization rate constants and branching ratios for the whole variety of the benzene dissociation products in molecular beam (collision-free) conditions. The calculations have been performed for different available internal energies, corresponding to one- and two-photon photoexcitations at different wavelengths including 248, 193, and 157 nm. For two-photon photoexcitations, the absorbed energy exceeds the ionization potential of benzene, 9.24 eV, and the molecule can decompose through dissociative ionization and vibronically induced autoionization. In this work, we limit our consideration only to the neutral hot benzene mechanism, for which the products would form line shape images in multimass ion imaging experiments. In order to predict the mechanism and product branching ratios for dissociative ionization, one has to investigate PES and decomposition pathways for $C_6H_6^+$ in a similar manner as for neutral benzene or benzene trication recently studied by us.[29] This task is beyond our goals in this work.

II. COMPUTATIONAL METHODS

The PES, different parts of which have been reported in our earlier publications,[20–23] was obtained using variations of the G2M method,[30] with geometries and vibrational frequencies of intermediates, transition states, and products obtained using the hybrid density functional B3LYP method[31] with the 6-311G** basis set. The optimized geometries (in Cartesian coordinates) of all species involved as well as their vibrational frequencies are given in the supplement to this paper.[32] These parameters were employed in our RRKM and VTST calculations.

In the RRKM theory (or quasiequilibrium theory),[33–35] rate constant $k(E)$ at an internal energy E for a unimolecular reaction $A^*\rightarrow A^{\#}\rightarrow P$ is expressed as

$$k(E)=\frac{\sigma}{h}\cdot\frac{W^{\#}(E-E^{\#})}{\rho(E)},$$

where σ is the reaction path degeneracy, h is Planck's constant, $W^{\#}(E-E^{\#})$ denotes the total number of states for the transition state (activated complex) $A^{\#}$ with a barrier $E^{\#}$, $\rho(E)$ represents the density of states of the energized reactant molecule A^*, and P is the product or products. We used the harmonic approximation to calculate the total number and density of states employing the direct count method.[36] In the calculations of the number of states for transition states we incorporated tunneling corrections using Miller's scheme where the shape of the barrier is approximated either by parabolic or Eckart potential.[37]

For the radical product channels, such as C_6H_5+H, $C_3H_3+C_3H_3$, $C_5H_3+CH_3$, or $C_4H_3+C_2H_3$, normally, no distinct transition state exists on the PES for the last reaction step, as it is a simple bond cleavage process. In such a case, we use the VTST approach[35] by considering different positions for the transition state along the reaction path, calculating rate constants corresponding to each of them and finding the minimal rate. In the microcanonical VTST, the minimum

in the microcanonical rate constant is found along the reaction path according to the following equation:

$$\frac{dk(E)}{dq^{\#}}=0,$$

where $q^{\#}$ is the reaction coordinate, so that a different transition state is found for each different energy. The reaction coordinates in our calculations were chosen as the lengths of breaking C–H or C–C bonds. The individual microcanonical rate constants are minimized at the point along the reaction path where the sum of states $W^{\#}(E-E^{\#})$ has a minimum. Each of these calculations requires values of the classical potential energy, zero-point energy, and vibrational frequencies as functions of the reaction coordinate.

We used the following procedure for the VTST calculations. At first, we calculated a series of energies at different distances between two dissociating fragments corresponding to the length of a bond to be broken during dissociation, which is considered as the reaction coordinate. To obtain these energies, we performed partial B3LYP/6-31G** geometry optimization with fixed values of the reaction coordinate and all other geometric parameters being optimized. Then we calculated $3N-7$ vibrational frequencies projecting the reaction coordinate out. Single-point energies for the optimized structures were refined at the coupled cluster[38] CCSD(T)/6-311G** level. Then, the CCSD(T)/6-311G** energies were multiplied by a scaling factor in order to match CCSD(T)/6-311G** and G2M energies of the final dissociation products. The scaling factor in this procedure was computed as the ratio of the relative energies of the products calculated at the G2M and CCSD(T)/6-311G** levels. For the C_6H_5+H channel, we additionally carried out similar calculations with scaling the CCSD(T)/6-311G** energy to the experimental energy of these products with respect to benzene, i.e., the experimental C–H bond energy. As the C–H bond energy obtained at the G2M level, 115.2 kcal/mol,[22,39] deviates by ~3 kcal/mol from the experimental value of 112.0 ± 0.6 kcal/mol,[40] this may affect the $C_6H_6 \rightarrow C_6H_5+H$ variational rate constants, especially, at low excitation energies. Finally, the variational transition states with the minimal values of the number of states were employed to calculate rate constants of the direct dissociation processes using the above RRKM formalism.

It should be noted that in the case in which the excitation energy is large and there exist low frequency modes, the harmonic approximation will not be accurate for low frequency modes in calculating these quantities and may introduce certain errors in our treatment. In order to take into account anharmonicity, more sophisticated RRKM calculations are required, but they are beyond the scope of the present work.

Under collision-free molecular beam conditions, kinetic master equations for unimolecular reactions can be expressed as follows:

$$\frac{d[C]_i}{dt}=\sum k_n[C]_j-\sum k_m[C]_i,$$

where $[C]_i$ and $[C]_j$ are concentrations of various intermediates or products, k_n and k_m are microcanonical rate constants computed as described above. The fourth order Runge–Kutta method[33–35] was used to solve the system of the master equations and to obtain numerical solutions for concentrations of various products vs time. The concentrations at the times when they have converged were used for calculations of product branching ratios. Additionally, we used the steady-state approximation to compute the branching ratios and obtained nearly identical results.

III. SUMMARY OF PES FOR VARIOUS DISSOCIATION AND ISOMERIZATION MECHANISMS

A. Atomic hydrogen elimination

The benzene molecule can split out a hydrogen atom to produce the phenyl radical, C_6H_5. As seen in Fig. 1, the calculated C–H bond energy in C_6H_6 (isomer **1**) is 115.2 kcal/mol at the G2M level, somewhat higher than the experimental value of 112 ± 0.6 kcal/mol.[40] The H-elimination occurs without an exit barrier. Additionally, the hydrogen loss can be preceded by migration of a hydrogen atom around the aromatic ring. A first 1,2-H shift leads from benzene (**1**) to a cyclohexadiene carbene intermediate *o*-C_6H_6 (**2**), where the CH_2 group is located in ortho position relative to the carbene carbon. The barrier for the hydrogen shift is 89.4 kcal/mol at the G2M level and **2** lies 88.8 kcal/mol above **1**. *o*-C_6H_6 can lose a hydrogen from the CH_2 group yielding the phenyl radical via a barrier of 33.2 and 121.4 kcal/mol relative to **2** and **1**, respectively. Another 2,3-H shift in **2** leads to *m*-C_6H_6 (**4**) or 1,4,6- (or 1,2,4-) cyclohexatriene, 77.3 kcal/mol above benzene. Elimination of a hydrogen atom from **4** again produces the phenyl radical with a barrier of 44.1 kcal/mol (121.4 kcal/mol with respect to benzene). Finally, a third 3,4-H shift leads from *m*-C_6H_6 to *p*-C_6H_6 (**5**), 92.9 kcal/mol higher in energy than **1**, which can be described as cyclohexadiene carbene with the CH_2 group in the para position relative to the carbene carbon. The barrier for the **4**→**5** rearrangement is 36.8 kcal/mol, 114.1 kcal/mol above benzene. The hydrogen loss from *p*-C_6H_6 occurs via a barrier of 121.6 kcal/mol relative to **1**. Thus, if hydrogen elimination takes place from a CH_2 group after one or more H migrations in benzene, the system has to overcome a barrier of 121–122 kcal/mol in order to produce the phenyl radical.

B. Molecular hydrogen elimination

The 1,2-H_2 elimination from benzene cannot occur, since a transition state for such process could not be found despite a careful search. Instead, 1,1-H_2 elimination takes place from isomer **2** and the H_2-loss is preceded by the 1,2-H shift in **1**. The H_2 elimination barrier is 33.2 and 121.4 kcal/mol relative to **2** and **1**, respectively. This reaction is less endothermic than the atomic hydrogen loss and the G2M computed heat of reaction, 86.4 kcal/mol, closely agrees with the experimental value of 85.2 kcal/mol.[41] H_2 elimination can also take place after additional hydrogen shifts, yielding *m*- and *p*-benzynes from the *m*-C_6H_6 and *p*-C_6H_6 intermediates **4** and **5**, respectively. The meta- and para- isomers of C_6H_4 are 14.3 and 27.2 kcal/mol less stable than

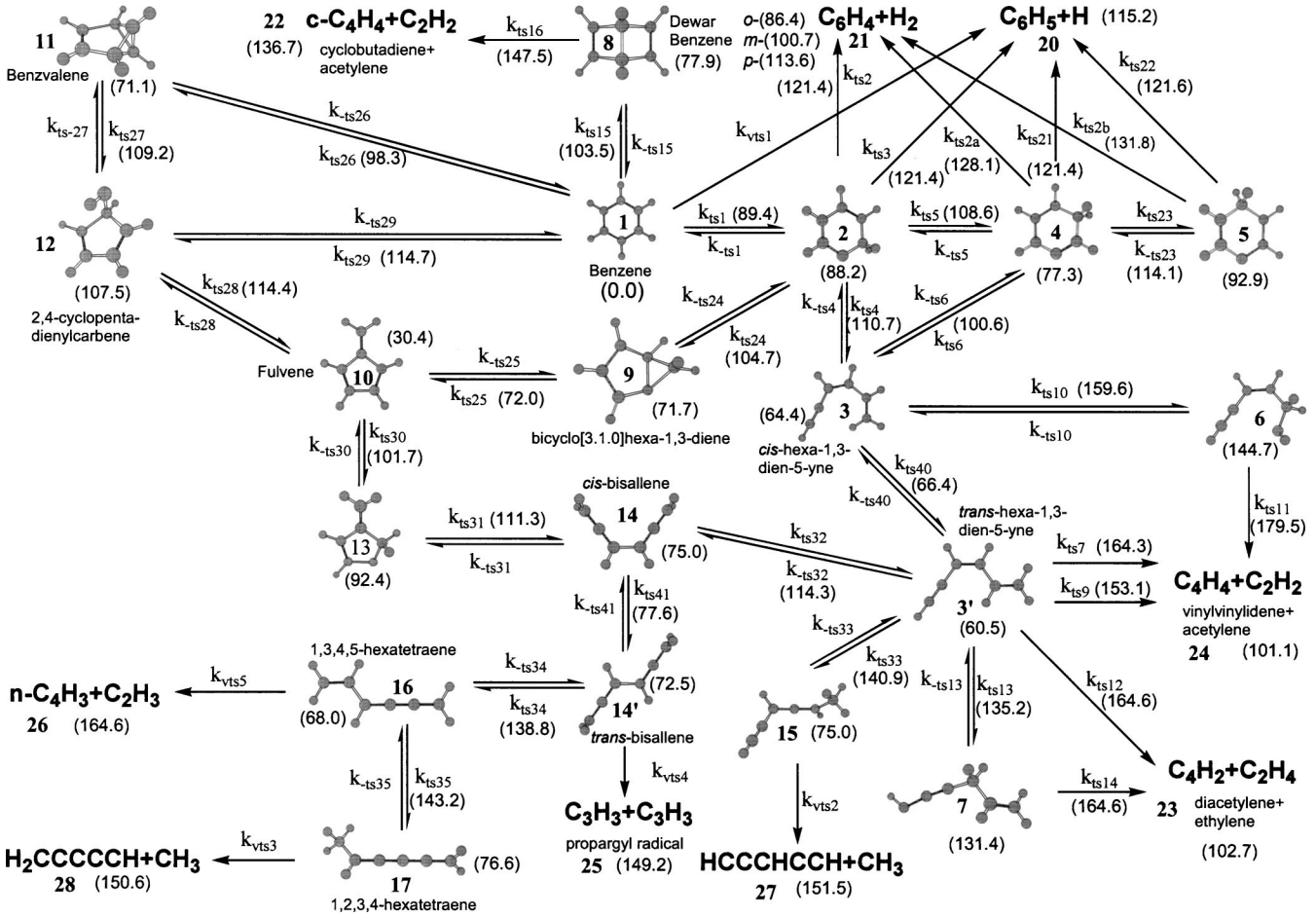

FIG. 1. Various reaction channels for isomerization and dissociation of benzene. Numbers in parentheses show energies relative to benzene (in kcal/mol, calculated at the G2M level) for intermediates, transition states, and products involved in the reaction.

o-benzyne.[42] As a result, the H_2 loss pathways leading to *m*-C_6H_4 and *p*-C_6H_4 from **4** and **5** have higher barriers of 128.1 and 131.8 kcal/mol relative to **1**, respectively, compared to 121.4 kcal/mol for the channel producing *o*-C_6H_4 from **2**. It should be noted that the energy of TS2b for the **5**→*p*-$C_6H_4+H_2$ reaction relative to TS2a for **4**→*m*-$C_6H_4+H_2$ was computed using the multireference configuration interaction MRCI(10,10)/6-311G** method.[43] We had to turn to the MRCI approach in this case because perturbative calculations of triple excitations in the CCSD(T) method failed for TS2b indicating a strong multireference character of the wave function for TS2b.

C. Cleavage of the carbon ring

Dissociation mechanisms leading to the formation of various hydrocarbon molecules and radicals involve cleavage of a C–C bond. The calculations show that this has to be preceded by rearrangement of the aromatic ring to a carbon chain. Aromaticity of benzene has to be destroyed before C_6H_6 can decompose to C_nH_m. A ring opening in cyclohexadiene carbene **2** leads to an acyclic isomer **3**, *cis*-hexa-1,3-dien-5-yne, via a barrier of 110.7 kcal/mol relative to benzene. During the **2**→**3** isomerization the ring opening is accompanied by a 1,2-hydrogen shift. **3** is 64.4 kcal/mol less stable than benzene. Another conformer, *trans*-hexa-1,3-dien-5-yne (**3′**), obtained by a facile rotation around the single C–C bond, is slightly more favorable, 60.5 kcal/mol relative to **1**. The isomer **3** can also be readily formed by the **4**→**3** rearrangement. The barrier for ring opening in **4** is relatively low, 23.3 kcal/mol. The energy of the **4**→**3** TS with respect to benzene is 100.6 kcal/mol, i.e., 10.1 kcal/mol lower than the energy of the **2**→**3** TS. Thus, the ring opening in benzene can occur by the following pathway: **1**→**2**→**4**→**3** with the highest barrier of 108.6 kcal/mol for the **2**→**4** step. The other pathways leading to the ring opening have slightly higher but comparable barriers: 110.7 kcal/mol for **1**→**2**→**3** and 111.3 kcal/mol for the mechanism involving fulvene, which will be described below.

Hexa-1,3-dien-5-ynes (**3** and **3′**) can eventually produce $C_4H_4+C_2H_2$ and $C_4H_2+C_2H_4$ by various mechanisms. In the first mechanism, the initial step is a 5,4-H migration to produce vinylvinylidene *v*-C_4H_4 and C_2H_2, which has a very high barrier, 103.8 and 164.3 kcal/mol above **3′** and **1**, respectively. The intermediate, *v*-C_4H_4, 139.0 kcal/mol higher in energy than benzene, can undergo H-migration to the more stable vinylacetylene C_4H_4 isomer with a barrier of 4.1 kcal/mol. The calculated endothermicity of the $C_6H_6 \rightarrow C_4H_4+C_2H_2$ reaction is 101.1 kcal/mol, in a satisfactory agreement with the experimental value of 104.8 kcal/mol.[41] Vinylacetylene can be also produced directly from **3′** by a

6,4-H migration via a somewhat lower barrier of 92.6 and 153.1 kcal/mol relative to **3′** and **1**, respectively. A stepwise mechanism involving two sequential 6,5- and 5,4-hydrogen shifts leads from **3** to $C_4H_4+C_2H_2$ via a carbene intermediate **6**, CH≡C–CH=CH–CH_2–CH. The highest barrier, 179.5 kcal/mol above **1**, occurs at the second step.

3 and **3′** can also decompose to C_4H_2 (diacetylene) and ethylene. The overall endothermicity for the C_6H_6 **1**→$C_4H_2+C_2H_4$ channel, 102.7 kcal/mol (103.7 kcal/mol in experiment[41]), is similar to that for $C_4H_4+C_2H_2$. **3′** can undergo a 4,5-H shift accompanied with a rupture of the bridged CC bond. The ethynylvinylidene structure, which seems to be produced as a result, is not a local minimum on the C_4H_2 PES and spontaneously rearranges to diacetylene, so the products are diacetylene and ethylene. The barrier is 164.6 and 104.1 kcal/mol relative to **1** and **3′**, respectively. Second possible channel leading to the same products, **3′**→**7**→$C_4H_2+C_2H_4$, involves two sequential 3,4- and 4,5-H migrations via the carbene intermediate **7**, CH–C≡C–CH_2–CH=CH_2. The higher barrier is found at the second step and it is similar to that for the one-step **3′**→$C_4H_2+C_2H_4$ decomposition, 164.6 kcal/mol above benzene. Thus, the barrier to produce $C_4H_2+C_2H_4$ from benzene is 11.5 kcal/mol higher than that for production of $C_4H_4+C_2H_2$.

A less stable isomer of C_4H_4, cyclobutadiene *c*-C_4H_4, can be formed from benzene with a slightly lower barrier than the more stable vinylacetylene. The pathway to *c*-C_4H_4 involves the isomerization of benzene **1** to Dewar benzene **8** via a barrier of 103.5 kcal/mol. At the second step, Dewar benzene (77.9 kcal/mol higher in energy than **1**) decomposes to *c*-C_4H_4 and acetylene with the barrier of 69.6 kcal/mol. The highest barrier on this pathway is 147.5 kcal/mol relative to benzene, i.e., 5.6 kcal/mol lower than the barrier leading to vinylacetylene. Meanwhile, the calculated endothermicity for the C_6H_6 **1**→*c*-$C_4H_4+C_2H_2$ reaction is 136.7 kcal/mol, 35.6 kcal/mol higher than that for the reaction giving vinylacetylene and acetylene.

D. Formation of various hydrocarbon radicals

Various hydrocarbon radicals can be produced by C–C bond cleavages in **3** and **3′** or in other chain isomers of C_6H_6 formed through isomerization of hexa-1,3-dien-5-ynes by sequential hydrogen shifts. Although various routes to the radical products exist, here we describe only the most favorable pathways (see Fig. 1). For instance, a 5,1-H shift in **3′** leads to a *cis*-bisallene intermediate **14** (1,2,4,5-hexatetraene, 75.0 kcal/mol above **1**) via a barrier of 53.8 and 114.3 kcal/mol, relative to **3′** and **1**, respectively. **14** can easily isomerize by rotation around the single C–C bond giving *trans*-bisallene **14′**, 2.5 kcal/mol more stable than the *cis*-conformer at the G2M level. In turn, **14′** undergoes a 4,2-H migration with a barrier of 66.3 kcal/mol to produce 1,3,4,5-hexatetraene **16**, 4.5 kcal/mol lower in energy than **14′**. The energy of the single C–C bond in 1,3,4,5-hexatetraene is 96.6 kcal/mol and its cleavage leads to the *n*-$C_4H_3+C_2H_3$ products, 164.6 kcal/mol above **1**.

The other radical products are propargyl radicals, C_3H_3. They can be formed by the single C–C bond cleavage in 1,2,4,5-hexatetraenes. The energy of this bond is calculated as 74.2 and 76.7 kcal/mol in **14** and **14′**, respectively, and the overall endothermicity of the C_6H_6 **1**→$C_3H_3+C_3H_3$ reaction is 149.2 kcal/mol. The most stable isomers of the C_5H_3 radical are $HCCCCCH_2$ and HCCCHCCH. These products can be formed by the following pathways: The 3,1-H shift to the CH_2 group in **16** gives 2,3,4,5- (or 1,2,3,4-) hexatetraene **17** (76.6 kcal/mol above **1**) via a barrier of 143.2 kcal/mol relative to benzene. The C–CH_3 single bond in **17** can be cleaved yielding the $HCCCCCH_2+CH_3$ products with overall endothermicity of 150.6 kcal/mol. On the other hand, the 4,6-H migration to CH_2 in **3′** produces 3,4-hexadien-1-yne (2,3-hexadien-5-yne) **15** through a barrier of 140.9 kcal/mol. **15** lies 75.0 kcal/mol above benzene and can decompose to $HCCCHCCH+CH_3$ by cleavage of the C–CH_3 bond. The HCCCHCCH isomer is only 0.9 kcal/mol higher in energy than $HCCCCCH_2$, so the total endothermicity of this dissociation channel is 151.5 kcal/mol.

E. Other isomerization pathways

The production of the tricyclic isomer of benzene, benzvalene (**11**), occurs through formation of two extra C–C bonds, so that the six-member aromatic ring converts into fused five-member and two three-member cycles. C_{2v}-symmetric benzvalene lies 71.1 kcal/mol at the G2M level and the isomerization barrier is 98.3 kcal/mol. The most favorable pathway leading from benzene to fulvene (**10**) involves the *o*-C_6H_6 intermediate **2**. From **2** the reaction proceeds by formation of a new C–C bond in the ring giving the bicyclo[3.1.0]hexa-1,3-diene intermediate **9**. The transition state connecting **2** and **9** resides 104.7 kcal/mol above benzene. **9** is very unstable kinetically and easily rearranges to **10** by the three-member ring opening via a barrier as low as 0.3 kcal/mol (72.0 kcal/mol relative to benzene). Fulvene is the second most stable isomer of C_6H_6 lying about 30 kcal/mol higher in energy than **1**. Fulvene can be also formed from benzvalene. **11** can first isomerize to 2,4-cyclopentadienylcarbene (**12**), which is 107.5 kcal/mol less stable than benzene, via a barrier of 109.2 kcal/mol with respect to **1**. Next, **12** undergoes a 1,2-H shift leading to fulvene via a barrier of 114.4 kcal/mol.

Fulvene undergoes the ring opening by a two-step mechanism. The first step is a 1,2-H shift between two ring carbons leading to intermediate **13**. The calculated barrier is 71.3 and 101.7 kcal/mol relative to fulvene and benzene, respectively, and **13** is 92.4 kcal/mol higher in energy than benzene. At the next step, the (CH_2=)C–CH_2 bond in the ring is cleaved with formation of *cis*-bisallene (1,2,4,5-hexatetraene) **14**. The highest barrier for the ring opening along the **10**→**13**→**14** pathway is 111.3 kcal/mol for the second step.

IV. RATE CONSTANTS AND PRODUCT BRANCHING RATIOS

Rate constants for individual reaction steps calculated using the RRKM theory and VTST are presented in Table I and product branching ratios obtained by solving the master equations are collected in Table II. In the calculations, we

TABLE I. RRKM and VTST calculated unimolecular rate constants (s^{-1}), reaction path degeneracies, and barrier heights (kcal/mol) of various reaction steps in photodissociation of benzene.

Rate constant	Reaction	Barrier height	Reaction path degeneracy	248 nm 115.2 kcal/mol	193 nm 148.1 kcal/mol	157 nm 182.1 kcal/mol	2×248 nm 230.6 kcal/mol	2×193 nm 296.2 kcal/mol
k_{ts1}	**1→ 2**	89.4	12	3.53×10^{4}	2.01×10^{7}	7.44×10^{8}	1.69×10^{10}	2.09×10^{11}
k_{-ts1}	**2→ 1**	1.2	2	5.80×10^{12}	7.75×10^{12}	8.87×10^{12}	9.84×10^{12}	1.06×10^{13}
k_{ts2}	**2→21**	33.2	1	1.10×10^{0}	1.22×10^{8}	6.44×10^{9}	8.22×10^{10}	4.48×10^{11}
k_{ts2a}	**4→21**	50.8	1	0	6.66×10^{5}	3.19×10^{8}	1.52×10^{10}	1.96×10^{11}
k_{ts2b}	**5→21**	38.9	1	0	6.42×10^{6}	3.37×10^{9}	1.20×10^{11}	1.17×10^{12}
k_{ts3}	**2→20**	33.2	2	3.32×10^{-2}	3.60×10^{8}	2.06×10^{10}	2.74×10^{11}	1.52×10^{12}
k_{ts4}	**2→ 3**	22.5	1	1.78×10^{7}	4.72×10^{10}	5.09×10^{11}	2.53×10^{12}	7.53×10^{12}
k_{-ts4}	**3→ 2**	46.3	1	8.54×10^{1}	3.19×10^{6}	1.28×10^{8}	1.80×10^{9}	1.17×10^{10}
k_{ts5}	**2→ 4**	20.4	2	6.65×10^{7}	1.71×10^{10}	1.16×10^{11}	4.29×10^{11}	1.07×10^{12}
k_{-ts5}	**4→ 2**	31.3	2	1.67×10^{6}	2.01×10^{9}	2.79×10^{10}	1.83×10^{11}	6.94×10^{11}
k_{ts6}	**4→ 3**	23.3	1	4.03×10^{8}	3.68×10^{10}	2.33×10^{11}	8.97×10^{11}	2.35×10^{12}
k_{-ts6}	**3→ 4**	36.2	1	7.68×10^{4}	2.11×10^{7}	2.40×10^{8}	1.50×10^{9}	5.67×10^{9}
k_{ts7}	**3′→24**	103.8	1	0	0	3.90×10^{1}	4.52×10^{6}	2.12×10^{9}
k_{ts9}	**3′→24**	92.6	1	0	1.74×10^{-9}	1.26×10^{3}	6.19×10^{6}	9.01×10^{8}
k_{ts10}	**3→ 6**	95.2	1	0	0	7.87×10^{1}	1.42×10^{6}	3.20×10^{8}
k_{-ts10}	**6→ 3**	14.9	2	0	0	2.55×10^{10}	6.64×10^{11}	2.66×10^{12}
k_{ts11}	**6→24**	34.8	2	0	0	4.03×10^{3}	1.93×10^{9}	8.25×10^{10}
k_{ts12}	**3′→23**	104.1	1	0	0	5.71×10^{0}	5.95×10^{5}	2.68×10^{8}
k_{ts13}	**3′→ 7**	74.7	1	0	1.39×10^{2}	1.60×10^{6}	3.48×10^{8}	1.14×10^{10}
k_{-ts13}	**7→ 3′**	3.8	2	0	3.03×10^{11}	1.23×10^{12}	2.18×10^{12}	3.00×10^{12}
k_{ts14}	**7→23**	33.2	2	0	1.43×10^{-8}	6.28×10^{6}	5.77×10^{9}	1.05×10^{11}
k_{ts15}	**1→ 8**	103.5	6	6.68×10^{0}	1.16×10^{5}	1.46×10^{7}	7.72×10^{8}	1.72×10^{10}
k_{-ts15}	**8→ 1**	25.6	1	8.29×10^{7}	1.54×10^{10}	1.22×10^{11}	5.50×10^{11}	1.60×10^{12}
k_{ts16}	**8→22**	69.6	2	0	7.92×10^{-1}	4.38×10^{7}	3.51×10^{10}	1.79×10^{12}
k_{ts21}	**4→20**	44.1	2	1.61×10^{-5}	4.72×10^{7}	5.85×10^{9}	1.38×10^{11}	1.16×10^{12}
k_{ts22}	**5→20**	28.7	2	3.11×10^{-1}	2.25×10^{9}	9.71×10^{10}	1.03×10^{12}	4.87×10^{12}
k_{ts23}	**4→ 5**	36.8	2	1.06×10^{4}	3.72×10^{8}	1.04×10^{10}	1.07×10^{11}	5.41×10^{11}
k_{-ts23}	**5→ 4**	21.2	4	1.32×10^{7}	4.55×10^{10}	4.46×10^{11}	2.04×10^{12}	5.76×10^{12}
k_{ts24}	**2→ 9**	16.5	1	6.84×10^{8}	4.48×10^{10}	2.03×10^{11}	5.77×10^{11}	1.19×10^{12}
k_{-ts24}	**9→ 2**	33.0	1	3.84×10^{6}	2.21×10^{9}	2.83×10^{10}	1.84×10^{11}	7.05×10^{11}
k_{ts25}	**9→10**	0.3	1	7.72×10^{12}	8.37×10^{12}	8.71×10^{12}	9.01×10^{12}	9.25×10^{12}
k_{-ts25}	**10→ 9**	41.6	2	1.92×10^{8}	3.21×10^{9}	1.71×10^{10}	7.38×10^{10}	2.40×10^{11}
k_{ts26}	**1→11**	98.3	12	3.39×10^{2}	1.35×10^{6}	1.08×10^{8}	4.18×10^{9}	7.53×10^{10}
k_{-ts26}	**11→ 1**	27.2	2	5.42×10^{8}	4.67×10^{10}	3.33×10^{11}	1.46×10^{12}	4.30×10^{12}
k_{ts27}	**11→12**	38.1	2	3.93×10^{5}	1.99×10^{9}	4.57×10^{10}	4.31×10^{11}	2.11×10^{12}
k_{-ts27}	**12→11**	1.7	2	2.92×10^{12}	8.83×10^{12}	1.16×10^{13}	1.37×10^{13}	1.54×10^{13}
k_{ts28}	**10→12**	84.0	2	9.51×10^{-3}	3.71×10^{4}	8.74×10^{6}	5.25×10^{8}	1.07×10^{10}
k_{-ts28}	**12→10**	6.9	1	4.93×10^{9}	7.74×10^{11}	2.09×10^{12}	3.84×10^{12}	5.72×10^{12}
k_{ts29}	**1→12**	114.7	12	5.94×10^{-4}	8.34×10^{3}	4.36×10^{6}	5.56×10^{8}	2.20×10^{10}
k_{-ts29}	**12→ 1**	7.2	2	7.07×10^{9}	1.27×10^{12}	3.41×10^{12}	6.22×10^{12}	9.15×10^{12}
k_{ts30}	**10→13**	71.3	2	1.32×10^{3}	4.58×10^{6}	2.35×10^{8}	5.53×10^{9}	6.14×10^{10}
k_{-ts30}	**13→10**	9.3	2	9.19×10^{10}	1.01×10^{12}	2.48×10^{12}	4.64×10^{12}	7.00×10^{12}
k_{ts31}	**13→14**	18.9	1	2.81×10^{7}	4.04×10^{10}	3.17×10^{11}	1.24×10^{12}	3.09×10^{12}
k_{-ts31}	**14→13**	36.3	2	1.04×10^{3}	1.59×10^{7}	3.61×10^{8}	3.17×10^{9}	1.44×10^{10}
k_{ts32}	**3′→14**	53.8	1	1.12×10^{0}	6.21×10^{5}	5.22×10^{7}	1.19×10^{9}	1.11×10^{10}
k_{-ts32}	**14→ 3′**	39.3	4	1.25×10^{2}	1.62×10^{7}	5.99×10^{8}	7.24×10^{9}	4.06×10^{10}
k_{ts33}	**3′→15**	80.4	1	0	1.41×10^{0}	1.17×10^{5}	5.33×10^{7}	2.67×10^{9}
k_{-ts33}	**15→ 3′**	65.9	3	0	3.24×10^{1}	1.21×10^{6}	2.94×10^{8}	8.99×10^{9}
k_{ts34}	**14′→16**	66.3	2	0	1.08×10^{2}	1.87×10^{6}	3.89×10^{8}	1.14×10^{10}
k_{-ts34}	**16→14′**	70.8	1	0	2.76×10^{1}	6.22×10^{5}	1.60×10^{8}	5.52×10^{9}
k_{ts35}	**16→17**	75.2	1	0	7.94×10^{-1}	1.38×10^{5}	6.61×10^{7}	3.11×10^{9}
k_{-ts35}	**17→16**	66.6	3	0	7.39×10^{0}	7.76×10^{5}	2.51×10^{8}	8.64×10^{9}
k_{ts40}	**3→ 3′**	2.0	1	1.35×10^{12}	1.68×10^{12}	1.92×10^{12}	2.13×10^{12}	2.30×10^{12}
k_{-ts40}	**3′→ 3**	5.9	1	9.03×10^{11}	1.56×10^{12}	2.15×10^{12}	2.78×10^{12}	3.39×10^{12}
k_{ts41}	**14→14′**	2.6	2	1.24×10^{12}	1.75×10^{12}	2.06×10^{12}	2.36×10^{12}	2.61×10^{12}
k_{-ts41}	**14′→14**	5.1	2	8.06×10^{11}	1.52×10^{12}	2.07×10^{12}	2.66×10^{12}	3.22×10^{12}
k_{vts1}[a]	**1→20**		6	1.91×10^{-4}	2.50×10^{4}	1.36×10^{7}	1.65×10^{9}	5.82×10^{10}
k_{vts1}[b]	**1→20**		6	4.75×10^{-2}	8.61×10^{4}	3.01×10^{7}	2.81×10^{9}	8.44×10^{10}
k_{vts2}	**15→27**		1	0	0	7.99×10^{6}	5.73×10^{9}	1.86×10^{11}
k_{vts3}	**17→28**		1	0	0	3.52×10^{6}	1.91×10^{9}	6.58×10^{10}
k_{vts4}	**14′→25**		1	0	0	4.96×10^{6}	2.99×10^{9}	1.25×10^{11}
k_{vts5}	**16→26**		1	0	0	1.62×10^{4}	2.61×10^{8}	2.31×10^{10}

[a]Variational $k(E)$ calculated assuming the C_6H_5+H dissociation limit to be 115.2 kcal/mol.
[b]Variational $k(E)$ calculated assuming the C_6H_5+H dissociation limit to be 112.0 kcal/mol.

TABLE II. Calculated product branching ratios in photodissociation of benzene.

Product		193 nm 148.1 kcal/mol	157 nm 182.1 kcal/mol	2×248 nm 230.6 kcal/mol	2×193 nm 296.2 kcal/mol
C_6H_5+H	**20**	99.59	97.51	79.85	62.81
$C_6H_4+H_2$	**21**	0.41	2.07	4.20	4.62
c-$C_4H_4+C_2H_2$	**22**	0	0.01	0.85	4.83
$C_4H_2+C_2H_4$	**23**	0	0	0.04	0.96
$C_4H_4+C_2H_2$	**24**	0	0	0.31	4.77
$C_3H_3+C_3H_3$	**25**	0	0.29	12.30	17.00
n-$C_4H_3+C_2H_3$	**26**	0	0.003	0.76	0.85
$HCCCHCCH+CH_3$	**27**	0	0.09	1.54	4.08
$H_2CCCCCH+CH_3$	**28**	0	0.02	0.15	0.08

used five different values of the initial internal energy for the ''hot'' benzene: 115.3 kcal/mol (absorption of a 248 nm photon), 148.1 kcal/mol (193 nm), 182.1 kcal/mol (157 nm), 230.6 kcal/mol (absorption of two 248 nm photons), and 296.2 kcal/mol (two 193 nm photons).

A. Variational rate constant for H elimination

Let us first pay our attention to the rate constant for the most significant decomposition channel, atomic hydrogen elimination from C_6H_6 **1**. As no distinct barrier exists for this channel, its rate constant was calculated using the microcanonical variational transition state theory. We performed the calculations assuming two different energies of the dissociating C–H bond, 115.2 (G2M value) and 112.0 kcal/mol (experimental value). As seen in Table I, at 248 nm the difference in rate constants computed for 115.2 and 112.0 kcal/mol exceeds two orders of magnitude. Such deviation stems from the fact that the available internal energy at 248 nm is only 0.1 kcal/mol in excess of the dissociation limit if this limit is 115.2 kcal/mol, but increases to 3.3 kcal/mol for the 112.0 kcal/mol limit. As the available energy increases, the differences in the rate constants computed with different dissociation limits diminish from two orders of magnitude for the available energy of 115.3 kcal/mol to factors of 3.44, 2.21, 1.70, and 1.45 for 148.1, 182.1, 230.6, and 296.2 kcal/mol, respectively. Thus, as the available energy increases, the rate constant becomes less sensitive with respect to small changes in the dissociation limit. For branching ratio calculations described in subsequent sections, we use the rate constants obtained with the dissociation limit of 112.0 kcal/mol.

B. Photodissociation at 248 nm

When benzene absorbs a 248 nm photon, the internal energy of the vibrationally excited ground state molecule formed after internal conversion (115.3 kcal/mol) is barely sufficient to produce the C_6H_5+H dissociation products. As shown in the previous section, the calculated rate constant k_{vts1} is very sensitive with respect to the dissociation limit. Taking this limit as 112.0 kcal/mol we obtained the dissociation rate as $4.75\times10^{-2}\,s^{-1}$, i.e., the lifetime of benzene in this case is in the range of 21 s. This is too long to be observable in molecular beam experiments. Indeed, recent measurements demonstrated that no dissociation occurs upon absorption of a 248 nm photon.[16] Ni and co-workers[16] gave the upper limit of the dissociation rate as $3\times10^3\,s^{-1}$ and the calculated value is significantly lower than this limit.

Among other decomposition products, $C_6H_4+H_2$ can be formed by tunneling through the barriers at TS2, TS2a, and TS2b, as the reaction endothermicities are lower but the barriers are higher than the available energy. However, the value of k_{ts2} calculated taking tunneling into account is only about $1\,s^{-1}$, which gives for the steady-state rate constant for the **1**→TS1→**2**→TS2→$C_6H_4+H_2$ reaction $[k(C_6H_4+H_2)=k_{ts1}\times k_{ts2}/(k_{-ts1}+k_{ts2})]$ a value lower than $10^{-8}\,s^{-1}$. Therefore, molecular hydrogen is not likely to be produced upon one-photon absorption at 248 nm. Isomerization reactions are also expected to be rather slow, as the calculated rate constants to form benzvalene and Dewar benzene are 3.4×10^2 and $6.7\,s^{-1}$ and the steady-state estimates of rate constants to produce fulvene $[k(\mathbf{10})=k_{ts1}\times k_{ts24}/(k_{-ts1}+k_{ts24})]$ and *cis*-1,3-hexadien-5-yne $[k(\mathbf{3})=k_{ts1}\times k_{ts4}/(k_{-ts1}+k_{ts4})]$ are 4.2 and $1.1\times10^{-1}\,s^{-1}$, respectively. On the other hand, hydrogen scrambling around the benzene ring, which can result in the H/D isotope exchange in deuterated benzenes, can occur on a microsecond scale through the **1**→**2**→**1** mechanism.

C. Photodissociation at 193 nm

For 193 nm, only the C_6H_5+H, $C_6H_4+H_2$, $C_4H_4+C_2H_2$, and $C_4H_2+C_2H_4$ channels are energetically allowed, while the other radical channels are forbidden. The transition states leading to the $C_4H_4+C_2H_2$ and $C_4H_2+C_2H_4$ products lie higher in energy than available 148.1 kcal/mol, therefore, these reactions can occur only by tunneling and the corresponding rate constants (see k_{ts9}, k_{ts11}, k_{ts12}, and k_{ts14} in Table I) are very low or zero. For the c-$C_4H_4+C_2H_2$ products, the barrier at TS16, 147.5 kcal/mol, is slightly lower than the available energy and k_{ts16} is also rather low, $7.9\times10^{-1}\,s^{-1}$. This leaves only C_6H_5+H and C_6H_4 (mostly ortho)$+H_2$ as possible products. The calculations indicate that H elimination dominates the reaction and from numerical solution of the master equations we obtained the $C_6H_5+H/C_6H_4+H_2$ branching ratio at 193 nm as 99.6/0.4. Although the branching ratios are not available from experiment so far, the molecular beams studies showed that C_6H_5+H are the major products at 193 nm, while a small amount of $C_6H_4+H_2$ can be also formed.[17] Using the steady-state approximation, we can compute the rate constants for H and H_2 elimination through various channels as well as the total rate constant of benzene decomposition to the C_6H_5+H and $C_6H_4+H_2$ products. As a result, we obtain $3.16\times10^2\,s^{-1}$ for the $C_6H_4+H_2$ channel, $8.61\times10^4\,s^{-1}$ for the direct H loss from **1**, $9.34\times10^2\,s^{-1}$ for the channel completed by H elimination from **2**, and 1.03×10^3 and $3.82\times10^2\,s^{-1}$ for the H eliminations from **4** and **5**, respectively. Thus, 97.3% of hydrogen atoms are produced directly from isomer **1** without an exit barrier, while 1.1%, 1.2%, and 0.4% are formed from **2**, **4**, and **5**, respectively, overcoming the exit barriers of ~6 kcal/mol. This explains why the experimental translational energy distribution of H atoms peaks near zero value (at 1.8 kcal/mol).[18] The total rate of benzene

decomposition to various products is computed as $8.89 \times 10^4\ s^{-1}$. The theoretical lifetime is thus ~11 μs, close to the experimental value of 10 μs.[16,18]

Rate constants for a number of isomerization channels are higher than those for H and H_2 loss. For instance, k_{ts1} for the **1**→**2** rearrangement is $2.01\times10^7\ s^{-1}$ and k_{ts1} for **2**→**1** is $7.75\times10^{12}\ s^{-1}$, which means that hydrogen scrambling around the benzene ring can occur in 50 ns, much faster than the lifetime of benzene at 193 nm. Therefore, the H/D isotope exchange in partially deuterated benzene can take place before these molecules dissociate. The rate of the benzene–benzvalene isomerization (**1**→**11**) is $1.35\times10^6\ s^{-1}$ indicating that carbon atoms can exchange their positions in the ring (potential $^{12}C/^{13}C$ isotope scrambling) in ~0.74 μs, again faster than the molecule can dissociate but slower than hydrogen exchange can occur. Assuming steady-state conditions, the rate constant for the benzene–fulvene rearrangement, which may result in both H and C isotope scrambling, can be estimated as $1.16\times10^5\ s^{-1}$. This rate is similar to that for the benzene-Dewar benzene (**8**) isomerization, also 1.16×10^5. Steady-state calculation of the rate constant for the ring opening to form structure **3** via isomer **2** gives $1.22\times10^5\ s^{-1}$. Thus, the **1**→**10**, **1**→**8**, and **1**→**3** isomerization channels are also somewhat faster than dissociation to C_6H_5+H. When experimental conditions are such that collisions are possible, benzene isomers can be collisionally deactivated and stabilized. Indeed, various studies of photochemistry of benzene showed that the main process is photochemical isomerization and the major products include benzvalene (**11**), fulvene (**10**), Dewar benzene (**8**), as well as *cis*- and *trans*-hexa-1,3-dien-5-ynes (**3** and **3′**).[5–14] Under collision-free conditions of molecular beams benzene has to dissociate in order to dissipate the excess energy.

D. Photodissociation at 157 nm

Photoexcitation by a 157 nm photon followed by eventual internal conversion into the ground electronic state produces hot benzene molecules with internal energy of 182.1 kcal/mol. In this case, all dissociation channels illustrated in Fig. 1 are open. However, calculations of the branching ratios show a relatively little change as compared to the results obtained for 148.1 kcal/mol (193 nm). Atomic hydrogen loss remains the dominant channel with the branching ratio of 97.5%. The branching ratio for H_2 elimination increases to 2.1%. Another molecular channel, c-$C_4H_4+C_2H_2$(0.01%), plays an insignificant role but might be observed. Of the radical product channels, $C_3H_3+C_3H_3$ exhibits the highest branching ratio (0.29%) followed by $C_5H_3+CH_3$(0.11%) and $C_4H_3+C_2H_3$(0.003%). Among the C_5H_3 isomers, HCCCHCCH is more likely to be produced (0.09%) than H_2CCCCCH(0.02%). Although the former is 0.9 kcal/mol less stable than the latter, the pathway to HCCCHCCH, **1**→**2**→**3**→**3′**→**15**→**27**, has fewer steps than that to H_2CCCCCH, **1**→**2**→**3**→**3′**→**14**→**14′**→**16**→**17**→**28**. In addition, intermediate **14′** can decompose to $C_3H_3+C_3H_3$, which makes the production of $H_2CCCCCH+CH_3$ less probable. Experimental branching ratios at 157 nm are not available until now but it is known that H elimination is the most important reaction channel.[18]

The absolute values of rate constants for various channels, including H and H_2 losses, significantly increase at 157 nm because the available internal energy rises by 34 kcal/mol. For instance, k_{vts1} for the direct H elimination from **1** shows a ~350-fold increase, from $8.61\times10^4\ s^{-1}$ at 193 nm to $3.01\times10^7\ s^{-1}$ at 157 nm. Steady-state approximation gives the total rates of $5.37\times10^5\ s^{-1}$ for the H_2 loss from **2** (~1700 times increase as compared to the 193 nm value) and 1.72×10^6, 1.87×10^6, and $5.95\times10^5\ s^{-1}$ for the H elimination from **2**, **3**, and **4**, respectively. Interestingly, in this case 87.8% of hydrogen atoms are eliminated directly from the benzene isomer **1** without passing over an exit barrier. The remaining amount, 5.0%, 5.5%, and 1.7% from **2**, **4**, and **5**, respectively, is formed with the exit barriers of 6.2–6.4 kcal/mol. These results can explain the experimental observation that the position of the peak in the translational energy distribution of the H atoms produced in photodissociation of benzene at 157 nm shifts significantly away from 0 to 3.2 kcal/mol.[18] The total rate constant for the C_6H_5+H channel is computed as $3.43\times10^7\ s^{-1}$, and the overall rate of benzene decomposition to various products is $3.48\times10^7\ s^{-1}$. This gives the lifetime of benzene for photodissociation at 157 nm as ~29 ns. The calculated lifetime is about 49 times lower than the experimental value of 1.4 μs. From 193 to 157 nm, the theoretical value of the lifetime decreases by a factor of ~400, while the experimental value shows only a sevenfold decrease. The dissociation of benzene at 157 nm was concluded to be most likely statistical,[18] therefore, non-RRKM behavior is not expected to cause this deviation between experimental and theoretical results. In the experimental study of benzene photodissociation at 157 nm, the lower instrumental limit for lifetime measurement was about 0.5 μs, so that the sensitivity of the setup with respect to faster decomposing species was low.[18] Apparently, new experimental measurements of the lifetime at 157 nm as well as a more advanced theoretical consideration would be required to reconcile the difference between theory and experiment.

E. Dissociation with higher internal energies

As benzene is photodissociated by the UV light it can absorb more than one photon and acquire higher internal energy after eventual internal conversion into the ground electronic states. In this case, a greater variety of products can be formed. For example, experimental studies of photodissociation at 193 nm showed that the $CH_3+C_5H_3$ and $C_2H_3+C_4H_3$ radical channels are originated from absorption of two photons[17,19] and the $C_6H_4+H_2$ channel can also have a two-photon character.[19] To analyze how the product branching ratios can change if two 248 or 193 nm photons are absorbed, we carried out RRKM and VTST calculations with the available internal energy of 230.6 and 296.2 kcal/mol.

As seen in Sec. IV B, if only one 248 nm photon is absorbed the decomposition reaction is very slow and is not likely to occur under conditions of molecular beam experiments. Alternatively, if the benzene molecule absorbs two photons it can decompose to various products with the calculated lifetime in the range of 0.3 ns. The C_6H_5+H channel

remains the most important one but the branching ratio decreases to 79.9%. Among the other channels, the most significant one is $C_3H_3+C_3H_3$(12.3%) followed by $C_6H_4+H_2$(4.2%), $CH_3+C_5H_3$(1.7%), c-$C_4H_4+C_2H_2$(0.85%), $C_4H_3+C_2H_3$(0.76%), $C_4H_4+C_2H_2$(0.31%), and $C_4H_2+C_2H_4$(0.04%). Assuming the internal energy of 296.2 kcal/mol corresponding to absorption of two 193 nm photons, we obtained the lifetime of benzene in the range of tens of picoseconds. The C_6H_5+H branching ratio then decreases to 62.8%, while that for $C_3H_3+C_3H_3$ rises to 17.0%. For the other channels, the calculated branching ratios also increase: $C_6H_4+H_2$(4.6%), $CH_3+C_5H_3$(4.2%), c-$C_4H_4+C_2H_2$(4.8%), $C_4H_3+C_2H_3$(0.9%), $C_4H_4+C_2H_2$(4.9%), and $C_4H_2+C_2H_4$(1.0%).

We emphasize here that for several reasons these results have only a qualitative character, even for dissociation of neutral hot benzene. First, with the energy increase anharmonicity can play a significant role not only for very-low-frequency modes and can introduce increasing errors to our RRKM and VTST calculations. Second, the mechanism of internal conversion into the ground electronic state from a high-lying excited state formed after absorption of two photons is not well understood. If the excited state energy is as high as 296 kcal/mol or about 12.8 eV, one cannot exclude that some excited state potential energy surfaces contribute to the photodissociation dynamics. In addition, at such high energies above the ionization potential of benzene (9.24 eV) the molecule can decompose through a dissociative ionization mechanism. Third, the dissociation time scale (ps) becomes comparable with the time required for the $S_1 \rightarrow S_0$ internal conversion. Thus, we can only suggest that in photodissociation of benzene after two-UV-photon absorption, among neutral products the H elimination channel is less dominant, the contribution of the other radical channels, especially $CH_3+C_3H_3$ and $CH_3+C_5H_3$, is significant, the $C_6H_4+H_2$ branching ratio remains in the range of ~2%–5%, and the other product channels can be also observable. This conclusion is in line with the experimental evidence.[17,19]

V. CONCLUSIONS

We have applied the *ab initio*/RRKM approach to investigate the photodissociation mechanism of benzene at various wavelengths upon absorption of one or two UV photons. As the dissociation takes place through the ''hot'' benzene mechanism on the ground state PES, reaction pathways leading to various decomposition products on this surface have been mapped out and then the RRKM theory have been applied to compute rate constants for individual reaction steps and kinetic master equations have been solved subsequently in order to predict branching ratios (relative yields) for a variety of potential products, including phenyl radical+H, o-benzyne+H_2, cyclobutadiene+acetylene, vinylacetylene+C_2H_2, 1,3-diacetylene+ethylene, propargyl radicals, $C_5H_3+CH_3$, and $C_4H_3+C_2H_3$. For the radical product channels, the microcanonical variational transition state theory has been used for calculations of rate constants for the final reaction steps, which involve single C–H or C–C bond cleavages and exhibit no distinct barriers.

The results demonstrate that upon absorption of a 248 nm photon dissociation is too slow to be observable in molecular beam experiments and the lifetime of benzene with respect to the C_6H_5+H decomposition channel is computed as ~21 s. Hydrogen scrambling around the benzene ring (H/D isotope exchange) occurs on a microsecond scale. In photodissociation at 193 nm, the dominant dissociation channel is H elimination to produce C_6H_5 and the minor reaction channel is H_2 elimination, with the branching ratio of 0.4%. The calculated lifetime of benzene at 193 nm is about 11 μs, in close agreement with the experimental value of 10 μs. At 157 nm, the H loss remains the dominant channel but its branching ratio decreases to 97.5%, while that for H_2 elimination increases to 2.1%. Other channels, $C_3H_3+C_3H_3$(0.29%), $C_5H_3+CH_3$(0.11%), c-$C_4H_4+C_2H_2$(0.01%), and $C_4H_3+C_2H_3$(0.003%), play insignificant role but might be observed. The lifetime is computed as ~29 ns, i.e., about 49 times shorter than the experimental estimate, and new experimental measurements of this quantity are encouraged. If benzene absorbs two UV photons and dissociates through the hot benzene mechanism, one can expect the C_6H_5+H channel would be less dominant, while the contribution of the other radical channels, $C_3H_3+C_3H_3$, $CH_3+C_5H_3$, and $C_4H_3+C_2H_3$, would significantly increase, and the $C_6H_4+H_2$ branching ratio would remain in the range of ~2%–5%. This prediction agrees with experimental observations[17,19] of the $CH_3+C_5H_3$, $C_4H_3+C_2H_3$, and $C_6H_4+H_2$ products when benzene is photodissociated by two 193 nm photons.

ACKNOWLEDGMENTS

We thank Academia Sinica and National Science Council of Taiwan, R.O.C., (Grant No. NSC 91-2113-M-001-029) for financial support. We are also grateful to Dr. C. K. Ni, Professor X. Yang, and Dr. J. J. Lin for stimulating discussions.

[1] C. E. Otis, J. L. Knee, and P. M. Johnson, J. Chem. Phys. **78**, 2091 (1983).
[2] N. Nakashima and K. Yoshihara, J. Chem. Phys. **77**, 6040 (1982).
[3] M. Sumitani, D. V. Oconnor, Y. Takagi, N. Nakashima, K. Kamogawa, Y. Udagawa, and K. Yoshihara, Chem. Phys. **93**, 359 (1985).
[4] M. A. Duncan, T. G. Dietz, M. G. Liverman, and R. E. Smalley, J. Phys. Chem. **85**, 7 (1981).
[5] K. Shindo and S. Lipsky, J. Chem. Phys. **45**, 2292 (1966).
[6] H. R. Ward and J. S. Wishnok, J. Am. Chem. Soc. **90**, 5353 (1968).
[7] P. Reilly and K. L. Kompa, J. Chem. Phys. **73**, 5468 (1980).
[8] W. Radloff, Th. Freudenberg, H.-H. Ritze, V. Stert, F. Noack, and I. V. Hertel, Chem. Phys. Lett. **261**, 301 (1996).
[9] Z. Min, R. Bersohn, and I. Oref, J. Chem. Phys. **93**, 5700 (1990).
[10] J. K. Foote, M. H. Mallon, and J. N. Pitts, J. Am. Chem. Soc. **88**, 3698 (1966).
[11] H. R. Ward, J. S. Wishnok, and P. D. Sherman, Jr., J. Am. Chem. Soc. **89**, 162 (1967).
[12] L. Kaplan and K. E. Wilzbach, J. Am. Chem. Soc. **89**, 1030 (1967).
[13] L. Kaplan, S. P. Walch, and K. E. Wilzbach, J. Am. Chem. Soc. **90**, 5646 (1968).
[14] F. Mellows and S. Lipsky, J. Phys. Chem. **70**, 4076 (1966).
[15] A. Yokoyama, X. Zhao, E. J. Hintsa, R. E. Continetti, and Y. T. Lee, J. Chem. Phys. **92**, 4222 (1990).
[16] S.-T. Tsai, C.-K. Lin, Y. T. Lee, and C.-K. Ni, J. Chem. Phys. **113**, 67 (2000).
[17] S.-T. Tsai, C.-L. Huang, Y. T. Lee, and C.-K. Ni, J. Chem. Phys. **115**, 2449 (2001).

[18] T. C. Hsu, J. Shu, Y. Chen, J. J. Lin, and X. Yang, J. Chem. Phys. **115**, 9623 (2001).
[19] T. C. Hsu, J. Shu, Y. Chen, J. J. Lin, and X. Yang, J. Chin. Chem. Soc. (Taipei) **49**, 1 (2001).
[20] L. K. Madden, A. M. Mebel, M. C. Lin, and C. F. Melius, J. Phys. Org. Chem. **9**, 801 (1996).
[21] A. M. Mebel, S. H. Lin, X.-M. Yang, S. H. Lin, and Y. T. Lee, J. Phys. Chem. A **101**, 3189 (1997).
[22] A. M. Mebel, M. C. Lin, D. Chakraborty, J. Park, S. H. Lin, and Y. T. Lee, J. Chem. Phys. **114**, 8421 (2001).
[23] A. M. Mebel, in *Reviews of Modern Quantum Chemistry*, edited by K. D. Sen (World Scientific, Singapore, 2002), p. 340.
[24] J. A. Miller and C. F. Melius, Combust. Flame **91**, 21 (1992).
[25] C. F. Melius, J. A. Miller, and E. M. Evleth, Proc. Combust. Inst. **24**, 621 (1992).
[26] H. F. Bettinger, P. R. Schreiner, H. F. Schaefer, and P. V. R. Schleyer, J. Am. Chem. Soc. **120**, 5741 (1998).
[27] J. A. Miller and S. J. Klippenstein, J. Phys. Chem. A **105**, 7254 (2001).
[28] J. A. Miller and S. J. Klippenstein, J. Phys. Chem. A **107**, 7783 (2003).
[29] T. S. Zyubina, G.-S. Kim, S. H. Lin, A. M. Mebel, and A. D. Bandrauk, Chem. Phys. Lett. **359**, 253 (2002); J. Theor. Comput. Chem. **2**, 205 (2003).
[30] A. M. Mebel, K. Morokuma, and M. C. Lin, J. Chem. Phys. **103**, 7414 (1995).
[31] (a) A. D. Becke, J. Chem. Phys. **98**, 5648 (1993); (b) C. Lee, W. Yang, and R. G. Parr, Phys. Rev. B **37**, 785 (1988).
[32] See Document No. E-JCPSA6-120-016415 for optimized geometries and vibrational frequencies, of all species involved in dissociation of benzene. A direct link to this document may be found in the online article's HTML reference section. The document may also be reached via the EPAPS homepage (http://www.aip.org/pubservs/epaps.html) or from ftp.aip.org in the directory /epaps/. See the EPAPS homepage for more information.
[33] H. Eyring, S. H. Lin, and S. M. Lin, *Basic Chemical Kinetics* (Wiley, New York, 1980).
[34] P. J. Robinson and K. A. Holbrook, *Unimolecular Reactions* (Wiley, New York, 1972).
[35] J. I. Steinfeld, J. S. Francisco, and W. L. Hase, *Chemical Kinetics and Dynamics* (Prentice–Hall, New Jersey, 1999).
[36] S. E. Stein and B. S. Rabinovitch, J. Phys. Chem. **58**, 2438 (1973).
[37] W. H. Miller, J. Am. Chem. Soc. **101**, 6810 (1979).
[38] (a) G. D. Purvis and R. J. Bartlett, J. Chem. Phys. **76**, 1910 (1982); (b) G. E. Scuseria, C. L. Janssen, and H. F. Schaefer III, *ibid.* **89**, 7382 (1988); (c) G. E. Scuseria and H. F. Schaefer III, *ibid.* **90**, 3700 (1989); (d) J. A. Pople, M. Head-Gordon, and K. Raghavachari, *ibid.* **87**, 5968 (1987).
[39] A. M. Mebel, M. C. Lin, T. Yu, and K. Morokuma, J. Phys. Chem. A **101**, 3189 (1997).
[40] G. E. Davigo, V. Bierbaum, C. H. DePuy, G. B. Ellison, and R. R. Squires, J. Am. Chem. Soc. **117**, 2590 (1995).
[41] NIST Chemistry WebBook, http://webbook.nist.gov/chemistry/, NIST Standard Reference Database Number 69-February, 2000 Release.
[42] R. Lindh, T. J. Lee, A. Bernhardsson, B. J. Persson, and G. Karlström, J. Am. Chem. Soc. **117**, 7186 (1995).
[43] H.-J. Werner and P. J. Knowles, J. Chem. Phys. **89**, 5803 (1988); P.-J. Knowles and H.-J. Werner, Chem. Phys. Lett. **145**, 514 (1988).